

The SDSS/XMM-Newton Quasar Survey: Correlation between X-ray spectral slope and Eddington ratio

G. Risaliti^{1,2}, M. Young^{1,3}, and M. Elvis¹

ABSTRACT

We present a correlation between the 2-10 keV spectral slope Γ_X and the Eddington ratio L/L_{EDD} in a sample of ~ 400 Sloan Digital Sky Survey quasars with available hard X-ray spectra from *XMM-Newton* serendipitous observations. We find that the Γ_X - L/L_{EDD} correlation is strongest in objects with black hole (BH) masses determined from the $H\beta$ line, and weaker (but still present) for those based on Mg II. An empirical non-linear correction of the Mg II-based masses, obtained by comparing the mass estimates in SDSS quasars having both $H\beta$ and Mg II measurements, significantly increases the strength of the correlation. No correlation is found among objects with BH masses derived from C IV, confirming that this line is not a reliable indicator of the BH mass. No significant correlation is found with the bolometric luminosity, while a Γ_X - M_{BH} relation is present, though with a lower statistical significance than between Γ_X and L/L_{EDD} . Our results imply a physical link between the accretion efficiency in the (cold) accretion disc of AGNs and the physical status of the (hot) corona responsible for the X-ray emission.

Subject headings: galaxies: active — X-rays: galaxies

1. Introduction

The origin of the X-ray emission in quasars is not well understood. In the widely accepted disk-corona model (Haardt & Maraschi 1993), the X-rays are produced in a hot phase (the corona) reprocessing the primary optical/UV emission of the disk. However, the mechanisms of energy transfer to the hot phase, and its geometry and size are not clear. Therefore, it is not known how the basic physical parameters (such as black hole mass, accretion rate, total luminosity) affect the X-ray emission. Laor et al. (1997) found a correlation between the soft X-ray (0.2-2 keV) slope and the full width at half maximum (FWHM) of the $H\beta$ emission line in a sample of 23 low redshift quasars, and suggested that the physical parameter driving the correlation is the Eddington ratio, L/L_{EDD} , where L is the bolometric luminosity. Further studies in the 2-10 keV energy band (e.g.

¹Harvard-Smithsonian Center for Astrophysics, 60 Garden Street, Cambridge, MA 02138, USA

²INAF-Osservatorio Astrofisico di Arcetri, Largo E. Fermi 5, I-50125 Firenze, Italy

³Boston University, Astronomy Department, 725 Commonwealth Ave., Boston, MA 02215, USA

Brandt et al. 1997, Shemmer et al. 2006) confirmed this correlation for the hard X-ray slope, and is therefore not related to the AGN “soft excess”. In particular, a Γ_X - L/L_{EDD} correlation has been found in a sample of ~ 150 SDSS quasars with *Chandra* spectra, and spanning a large redshift range (Kelly et al. 2008). Recently Shemmer et al. (2008) presented a similar analysis based on a sample of 35 quasars, spanning more than three orders of magnitude in luminosity, and obtained a stronger correlation between Γ_X and the Eddington ratio L/L_{EDD} than with $\text{FWHM}(H\beta)$, breaking the partial degeneracy between these two quantities. The main limitation of past studies involving X-ray slopes is that either they rely on low quality X-ray data, or they are based on relatively small samples. The availability of large, homogeneous samples of quasars with high quality optical and X-ray spectral data is now opening new possibilities in this field.

In particular, we recently obtained a new sample of ~ 800 quasars within the SDSS/*XMM-Newton* survey (Risaliti & Elvis 2005, Young, Elvis & Risaliti 2009, hereafter Y09) obtained by cross-correlating the SDSS DR5 quasar catalog with the *XMM-Newton* public archive. Since we only selected serendipitous *XMM-Newton* observations, this sample can be considered as randomly extracted from the SDSS quasars. About 500 quasars in this sample have good enough X-ray data to perform a basic spectral analysis and obtain a continuum slope. A complete description of the survey, with an analysis of the general properties of the sample, is presented in Y09.

The simultaneous availability of optical/UV and X-ray spectra not only allows a more precise analysis of the α_{OX} -luminosity correlation (this subject is developed in a companion paper, Young, Risaliti & Elvis 2009, in prep.), but also opens a whole new field of analysis of the possible correlations among X-ray spectral parameters, optical/UV continuum and line emission, and physical parameters of the AGN.

Here we extend the analysis of the correlation between Γ_X and optically-derived and global quantities such as M_{BH} , L/L_{EDD} , and L for our sample of SDSS-*XMM-Newton* quasars, consisting of more than 400 objects.

2. The sample

Our sample is taken from the SDSS/*XMM-Newton* quasar survey (Y09). Since we are interested in a homogeneous analysis of X-ray slopes, we excluded radio loud (RL) quasars and broad absorption line (BAL) quasars, whose X-ray spectra may be contaminated by synchrotron emission (in RLs) or affected by heavy absorption (in BALs). Since a complete removal of BALs is possible only for sources at $z > 1.5$, and \sim half of our sources have $z < 1.5$, there may be some residual BALs contamination in our sample. By removing objects with flat X-ray spectra (see below) we expect to further clean the sample from BALs, which are typically harder in X-rays than non-BAL quasars (e.g. Gallagher et al. 2006). The remaining spurious objects are expected to be $\lesssim 5\%$ of the sample.

For the 403 quasars with a signal-to-noise ratio $S/N > 6$, we used the available X-ray and optical/UV spectral data to obtain estimates of the relevant physical parameters for our analysis:

the X-ray continuum slope, Γ_X , the black hole mass, M_{BH} , and the bolometric luminosity, L_{BOL} . The sample spans about three orders of magnitude in optical luminosity (this can be estimated from the bottom panel of Fig. 1, where we show the bolometric luminosities, which are roughly proportional to the optical ones, as explained below). The 2-10 keV luminosities range from 10^{43} to $10^{45.5}$ erg s $^{-1}$ for most sources, with small tails down to 10^{42} erg s $^{-1}$ at $z < 0.5$, and up to 10^{46} erg s $^{-1}$ at $z > 1.5$. More details on the luminosity distribution can be found in Y09.

The X-ray slopes Γ_X were obtained from basic power law plus Galactic absorption models applied to the spectral data in the rest-frame 2-10 keV band. The data reduction was performed with the SAS package¹ following the standard recommended steps in the *XMM-Newton* Science Data Center web page. The analysis was made with the *Sherpa* analysis package². All the details about the data reduction and analysis are presented in Y09. The sample spans an X-ray luminosity 10^{43} erg s $^{-1} < L_X < 5 \times 10^{46}$ erg s $^{-1}$, and a redshift range $0.1 < z < 4.5$.

The black hole masses have been estimated (Shen et al. 2008, hereafter S08) from the widths of the optical broad emission lines and the underlying continuum luminosity. Three different optical lines are used, depending on the redshift of the sources: $H\beta$ ($0 < z < 0.9$), Mg II ($0.4 < z < 2.2$), and C IV ($1.7 < z < 4.5$). When the black hole masses from two different lines are available, we prefer $H\beta$ over Mg II, and Mg II over C IV (see Section 4 for more details on this issue). For the $H\beta$ and Mg II lines, the widths were obtained through a two-Gaussian fit, after subtracting a template reproducing the Fe II emission. The adopted templates are those of Boroson & Green (1992) for the $H\beta$ line and of Salviander et al. (2007) for the Mg II line. For the C IV line, the continuum has been fitted with a simple power law, while the line FWHM has been estimated from the analytic three-Gaussian fit described in Laor et al. (1994). Full details on the optical spectral analysis are described in S08.

The bolometric luminosities are derived from the continuum monochromatic luminosity at the line wavelength, adopting a correction based on an analytical intrinsic Spectral Energy Distribution (SED). The optical to UV SED is approximated by three power laws with spectral indexes (in a $\nu - f_\nu$ plane) $\alpha_1 = -2$ in the 1-10 μm interval³, $\alpha_2 = -0.44$ from 1 μm to 1,200 \AA , and $\alpha_3 = -1.76$ from 1,200 \AA to 500 \AA , in agreement with the average SED of SDSS quasars (Richards et al. 2006). The X-ray luminosity is modeled with a power law continuum with the observed photon index, starting at 0.1 keV, and an exponential decrease with a cut-off energy $E_C = 100$ keV. The X-ray to optical ratio is directly obtained from the observed data.

We analyzed the correlation between the X-ray photon index, Γ_X , and: (1) the Eddington

¹<http://xmm.esac.esa.int/sas/8.0.0/>

²<http://cxc.harvard.edu/sherpa/>

³This part gives a negligible contribution, and represents the Raileigh-Jeans tail of the accretion disk emission. The actual observed emission at wavelengths $\lambda > 1 \mu\text{m}$ is due to reprocessing by dust, and therefore is not included here.

ratio, L/L_{EDD} , (2) the bolometric luminosity, L_{BOL} , and (3) the black hole mass, M_{BH} . The main results for the whole sample are shown in Fig. 1. As mentioned above, our data consist of three different subsamples, depending on the line used to estimate the black hole mass. There are at least two reasons to perform a separate analysis for each subsample: (1) the black hole mass-line width correlation is directly calibrated using reverberation mapping on $H\beta$ widths (e.g. Peterson et al. 2004), while it is indirectly calibrated using $H\beta$ for the other lines (Vestergaard et al. 2006); (2) the luminosity and redshift ranges spanned by the three lines are quite different (Fig. 1, bottom panel), and a possible luminosity dependence has to be considered. We therefore repeated the same analysis for the total sample and each of the three subsamples.

3. Statistical Analysis

Our statistical analysis consists of several steps and checks. We first performed a non-parametric Spearman rank test on each correlation, followed by a least squares linear fit. In order to take into account the effect of possible deviant points, we performed the above analysis with different selections based on the quality of X-ray data:

(1) We tried different cuts in signal-to-noise of the X-ray spectra ($6 < S/N < 10$), and in quality of the fit of the X-ray data ($0.5 < \chi^2_{\nu} < 2$). No significant dependence on these choices has been found. The final analysis was performed on objects with $S/N > 8$ in the X-ray spectra (see Y09 for details) and $\chi^2_{\nu} < 1.5$ in the X-ray fit.

(2) We excluded possibly “bad” points, i.e. those with extreme best fit values of Γ_X ($\Gamma_X > 3$ or $\Gamma_X < 1$), or large deviations from the best fit in a statistical sense ($(\Gamma_X - \langle \Gamma_X \rangle) / \Delta \Gamma_X > 5$). Again, the results remain consistent for all the different cuts.

(3) We estimated the errors for the slope m and intercept q through a bootstrap analysis, consisting of repeating the linear fits on randomly selected sets of data drawn from our sample, allowing for repetitions. This technique takes into account strongly deviating points that could affect the correlations.

All these checks demonstrate that our results are stable and do not depend on single deviating points.

The results for the total sample are shown in Table 1. The final sample contains 343 objects. The subsamples consist of 82 ($H\beta$), 290 (Mg II) and 58 (C IV) data points. 58 objects have both $H\beta$ and Mg II measurements, while 29 have both MG II and C IV.

4. Results

We found a highly statistically significant correlation (probability of null correlation $P < 0.1\%$) between the X-ray slope and the Eddington ratio L/L_{EDD} , and a weaker, but still significant anti-correlation between Γ_X and the black hole mass. No significant trend ($P > 5\%$) is found with the

Table 1: Results of the correlation analysis

Sample/Corr.	N ^a	P ^b	m ^c	q ^d	Disp ^e	r ^f
Total: Γ_X -L/ L_{EDD}	343	$< 10^{-8}$	0.31 ± 0.06	1.97 ± 0.02	0.33	0.32
$H\beta$: Γ_X -L/ L_{EDD}	82	$< 10^{-8}$	0.58 ± 0.11	1.99 ± 0.04	0.35	0.56
$MgII$: Γ_X -L/ L_{EDD}	290	3×10^{-4}	0.27 ± 0.09	1.88 ± 0.03	0.33	0.21
$MgII$ (corr) ^g : Γ_X -L/ L_{EDD}	290	3×10^{-6}	0.24 ± 0.05	1.98 ± 0.02	0.32	0.30
CIV : Γ_X -L/ L_{EDD}	58	0.47	-0.11 ± 0.17	2.03 ± 0.06	0.27	-0.13
Total: Γ_X - M_{BH}	343	0.004	-0.22 ± 0.08	1.981 ± 0.03	0.35	-0.16
$H\beta$: Γ_X - M_{BH}	82	0.003	-0.33 ± 0.10	1.95 ± 0.04	0.39	-0.35
$MgII$: Γ_X - M_{BH}	290	6×10^{-4}	-0.11 ± 0.03	2.01 ± 0.03	0.33	-0.21
CIV : Γ_X - M_{BH}	58	0.04	0.27 ± 0.10	1.77 ± 0.08	0.26	0.27
Total: $\Gamma_X - L_{BOL}$	343	0.45	0.03 ± 0.04	1.90 ± 0.04	0.35	0.04
$H\beta$: $\Gamma_X - L_{BOL}$	82	0.12	0.22 ± 0.15	1.91 ± 0.05	0.41	0.06
$MgII$: $\Gamma_X - L_{BOL}$	290	0.10	-0.05 ± 0.04	2.02 ± 0.03	0.34	-0.07
CIV : $\Gamma_X - L_{BOL}$	58	0.06	0.23 ± 0.10	1.70 ± 0.14	0.27	0.20

^a: Number of object in each sample. 58 objects have both $H\beta$ and Mg II measurements, while 29 have both Mg II and C IV. ^b: Probability of a null correlation from a Spearman’s test. ^c, ^d: slope m and intercept q of a best fit linear correlation $Y = m \times (X - X_0) + q$. In all the correlations $Y = \Gamma_X$. The independent variable X and the reference point X_0 are: $X = \log(L/L_{EDD})$, $X_0 = -1$ for the Γ -L/ L_{EDD} correlation, $X = \log(M_{BH}/M_{\odot})$, $X_0 = 8.5$ for the Γ - M_{BH} correlation, and $X = \log(L_{BOL}/10^{44} \text{ erg cm}^2 \text{ s}^{-1})$, $X_0 = 1.5$ for the Γ - L_{BOL} correlation. ^e: Dispersion of the data points with respect to the linear correlation. ^f: linear correlation coefficient. ^g: Values obtained adopting the correction for Mg II based masses discussed in Section 3 and Fig. 3.

bolometric luminosity (Table 1). Separate analysis of the subsamples show that the Γ_X -L/ L_{EDD} correlation is strongest for objects whose M_{BH} is determined from $H\beta$ (Fig. 2), weaker for Mg II objects, and absent for C IV objects. The linear correlation coefficient is higher than 0.5, conventionally considered the threshold for a “strong” correlation, only for the Γ_X -L/ L_{EDD} correlation in the $H\beta$ group.

Since $L/L_{EDD} \propto M_{BH}^{-1}$, and $M_{BH} \propto \text{FWHM}^2 L^\alpha$ ($\alpha = 0.52 \pm 0.04$ in the calibration of Bentz et al. 2006), a strong Γ_X -L/ L_{EDD} correlation may be due to an intrinsic correlation between Γ_X and FWHM. We tested this possibility and found a highly significant Γ_X -FWHM correlation (slightly weaker than the Γ_X -L/ L_{EDD} one in the total and $H\beta$ samples). As a more general approach, we tested correlations of the form $\text{FWHM}^{-2} \times L^\beta$ varying the exponent β in the interval 0-0.8, and we always found the same level of correlation for any value of β (null correlation probability $P < 10^{-8}$, linear correlation coefficient r in the range 0.53-0.60). This confirms that the luminosity term does not contribute to the observed correlation. This may be due to either a physical independence of these quantities, or to a too narrow luminosity range in our sample (Fig. 1). We note that Shemmer et al. (2008) claim a stronger dependence of Γ_X on L/ L_{EDD} than on FWHM($H\beta$) for their quasar sample, which is smaller (35 objects) but spanning a larger luminosity interval.

The Γ_X - $\log(M_{BH})$ relation is statistically significant (Table 1), but rather weak, with a slope of ~ 0.3 . Since $L_{EDD} \propto M_{BH}$, some degree of correlation of Γ_X with M_{BH} is expected, given the strength of the Γ_X -L/ L_{EDD} correlation. Formally, it is not possible to remove this partial degeneracy. We only note that the stronger Γ_X -L/ L_{EDD} correlation suggests that this is the physically relevant relation, and, therefore, that there is no independent support for a direct physical dependence of Γ_X on M_{BH} .

The decreasing strength (in terms of slope of a linear correlation) and statistical significance of the correlation going from $H\beta$ - to Mg II to C IV-estimated FWHM black hole masses could be due to the different average luminosities of the three subsamples (Fig. 1, bottom panel), or could be due to a problem related to the estimates of M_{BH} . We directly explored both possibilities:

- **Luminosity effects.** The luminosity intervals of the three subsamples overlap significantly. We analyzed the Γ_X -L/ L_{EDD} correlation for luminosity-limited subsamples of the Mg II group, matched to the luminosity distribution of the $H\beta$ group. We performed Pearson’s tests and linear correlation fits for Mg II objects with bolometric luminosities $\log(L_{BOL}) < 45.5$ (23 objects), $\log(L_{BOL}) < 45.8$ (76 objects), and $\log(L_{BOL}) < 46$ (123 objects). In no case did we find a better correlation than in the whole Mg II sample. This suggests that luminosity is not the main reason for the observed trend.

- **Black hole mass estimates.** We compared the black hole mass estimates from pairs of lines in the S08 sample. As discussed in S08, about 8,000 objects in their sample have black hole mass estimates from both $H\beta$ and Mg II, and about 5,000 from both Mg II and C IV. In Fig. 3 we plot the mass estimates for the two groups (this plot is analogous to Fig. 6 in S08), with a best fit linear correlation. We find a strong (though not linear) correlation between $H\beta$ and Mg II masses, while no significant correlation is found between Mg II and C IV masses. These two findings have two

different possible explanations:

- Both $H\beta$ and Mg II are expected to be produced by virialized gas, and are therefore in principle good mass indicators. The mismatch between $H\beta$ and Mg II masses is likely related to the uncertainties in the measurement of the Mg II line parameters: the line is a doublet, and the estimate of the strength of the contaminating Fe II emission is more problematic than for the $H\beta$ line. Recently Onken & Kollmeier (2008) discussed this issue and found that a correction has to be applied to the average Mg II based mass distribution, in order to make it compatible with the one based on $H\beta$. In our case, in order to apply a correction to the Mg II-based values of M_{BH} in single sources, we used the best fit linear correlation shown in Fig. 3A ($\log[M_{BH}(H\beta)] = 1.8 \times \log[M_{BH}(Mg II)] - 6.8$), under the assumption that the $H\beta$ -based masses are correct. This should improve the precision of the estimates of M_{BH} , at least in a statistical sense. We repeated the same statistical analysis on the so-modified Mg II subsample, and we obtained a stronger correlation (probability of null correlation $< 10^{-6}$), and a linear correlation coefficient $r=0.30$. This is still lower than that found for $H\beta$ sample, as expected, since our correction is only statistical, and a significant residual dispersion is still present between the $H\beta$ -based and Mg II-based estimates (Fig. 3, upper panel). However, the strength of the correlation is significantly higher than that found with the original M_{BH} values ($r=0.21$, Table 1).

- C IV is a high ionization line, produced in the inner broad line region by gas probably having non-virialized components (for example, associated to an outflow). This makes this line a poor estimator of the black hole mass (Baskin & Laor 2005, Netzer et al. 2007). The lack of correlation between Mg II and C IV masses confirms this finding, and provides an explanation for the absence of correlations between the X-ray spectral slope and the Eddington ratio and the black hole mass.

5. Conclusions

We presented a strong correlation between the X-ray photon index, Γ_X , and the Eddington ratio, L/L_{EDD} for a sample of ~ 400 AGNs having good quality X-ray and optical spectra from the SDSS quasar survey and serendipitous *XMM-Newton* observations. A weaker, but statistically significant, correlation between Γ_X and the black hole mass M_{BH} was also found.

The correlations found here are important in two respects: first, a Γ_X - L/L_{EDD} correlation is an important constraint for theoretical emission models. In general, it suggests a strong link between the accretion rate and the physical conditions in the hot corona producing the X-rays. For example, recently Cao (2008) showed that a Γ_X - L/L_{EDD} relation, together with the α_{OX} -luminosity relation, depend on the balance between the magnetic field and the gas and electron pressures in a disc-corona model where the corona is heated by magnetic field reconnections.

Second, as already pointed out by Shemmer et al. (2008), our results show that the X-ray slope can be used as an Eddington ratio estimator. Since the X-ray luminosity can be converted to a total luminosity through bolometric corrections and the α_{OX} -luminosity correlation, an estimate of the black hole mass can be obtained from the X-ray data alone. Given the high dispersion of

the correlation (0.4 dex), this is not at present a reliable method for single sources. However, it could be a powerful technique when used to estimate average values in large samples, such as the ones which are expected to be available in the future from new missions like E-Rosita.

We are currently working at expanding SDSS-XMM quasar survey, using the DR7 version of the SDSS⁴ and the 2009 *XMM-Newton* archive. This new sample will have about twice as many quasars with good quality X-ray spectra, and will allow further investigations of the multi-wavelength correlations among AGNs.

We are grateful to the referee for his/her constructive comments. This work has been partly supported by grants prin-miur 2006025203, ASI-INAF I/088/06/0, and NASA NNX07AI22G.

REFERENCES

- Baskin, A., & Laor, A. 2005, MNRAS, 356, 1029
- Bentz, M. C., Peterson, B. M., Pogge, R. W., Vestergaard, M., & Onken, C. A. 2006, ApJ, 644, 133
- Boroson, T. A., & Green, R. F. 1992, ApJS, 80, 109
- Brandt, W. N., Mathur, S., & Elvis, M. 1997, MNRAS, 285, L25
- Cao, X. 2008, arXiv:0812.1828
- Haardt, F., & Maraschi, L. 1993, ApJ, 413, 507
- Kelly, B. C., Bechtold, J., Trump, J. R., Vestergaard, M., & Siemiginowska, A. 2008, ApJS, 176, 355
- Laor, A., Bahcall, J. N., Jannuzi, B. T., Schneider, D. P., Green, R. F., & Hartig, G. F. 1994, ApJ, 420, 110
- Laor, A., Fiore, F., Elvis, M., Wilkes, B. J., & McDowell, J. C. 1997, ApJ, 477, 93
- Netzer, H., Lira, P., Trakhtenbrot, B., Shemmer, O., & Cury, I. 2007, ApJ, 671, 1256
- Onken, C. A., & Kollmeier, J. A. 2008, ApJ, 689, L13
- Peterson, B. M., et al. 2004, ApJ, 613, 682
- Richards, G. T., et al. 2006, ApJS, 166, 470

⁴<http://www.sdss.org/DR7/>

- Risaliti, G., & Elvis, M. 2005, *ApJ*, 629, L17
- Salviander, S., Shields, G. A., Gebhardt, K., & Bonning, E. W. 2007, *ApJ*, 662, 131
- Shemmer, O., Brandt, W. N., Netzer, H., Maiolino, R., & Kaspi, S. 2006, *ApJ*, 646, L29
- Shemmer, O., Brandt, W. N., Netzer, H., Maiolino, R., & Kaspi, S. 2008, *ApJ*, 682, 81
- Shen, Y., Greene, J. E., Strauss, M. A., Richards, G. T., & Schneider, D. P. 2008, *ApJ*, 680, 169 (S08)
- Steffen, A. T., et al. 2006, *AJ*, 131, 2826
- Vestergaard, M., & Peterson, B. M. 2006, *ApJ*, 641, 689
- Young, M., Elvis, M., & Risaliti, G. 2008, *ApJ*, 688, 128
- Young, M., Elvis, M., & Risaliti, G. 2009, arXiv:0905.0496

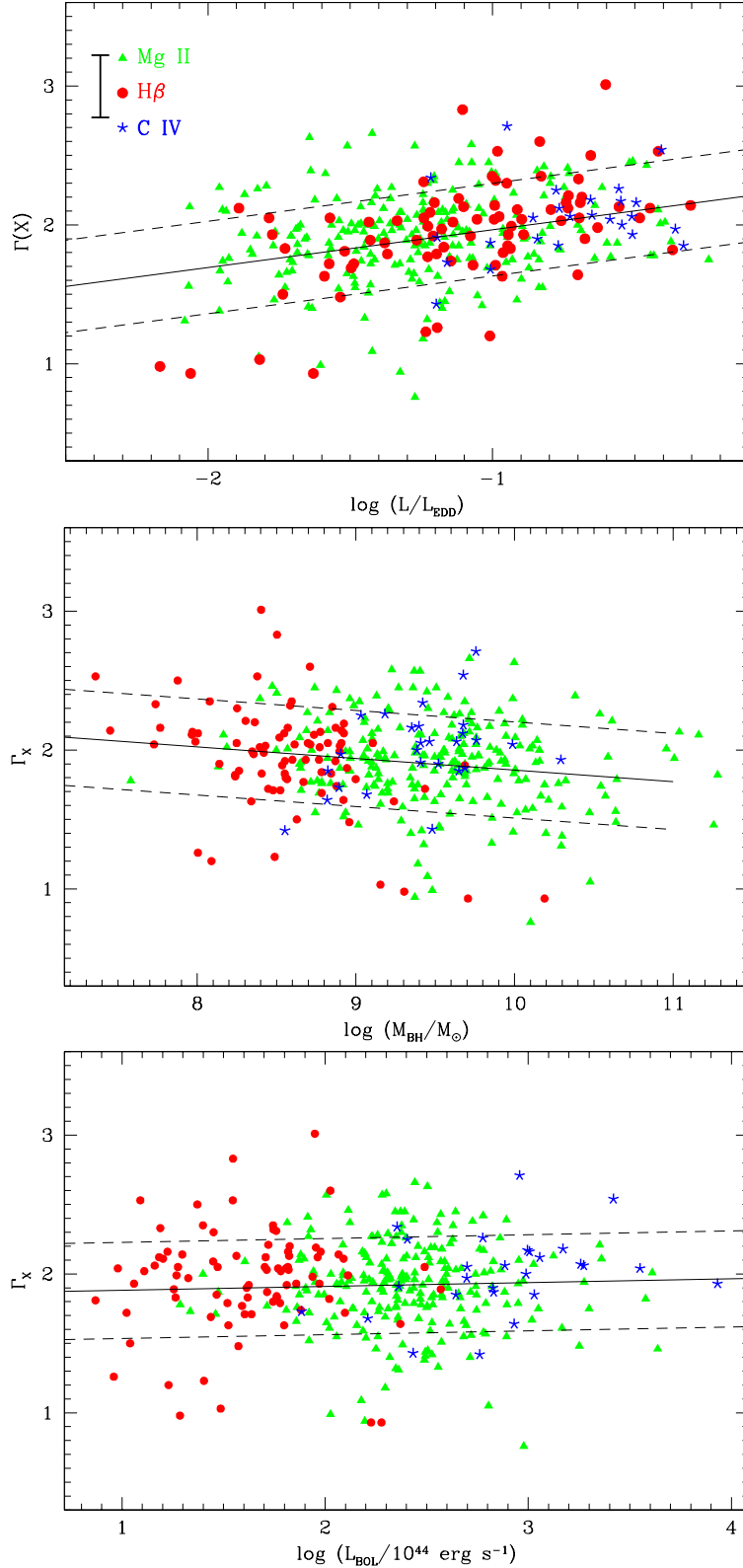


Fig. 1.— Correlations between Γ_X and L/L_{EDD} , M_{BH} , and L_{BOL} for our sample. The error bars are not shown for clarity. A typical error is shown in the top panel. The three colors refer to the line used to estimate the black hole mass. The lines show the best linear fits and the dispersions. The statistical errors on the slopes are small with respect to the dispersions, as shown in Table 1, and are not plotted here.

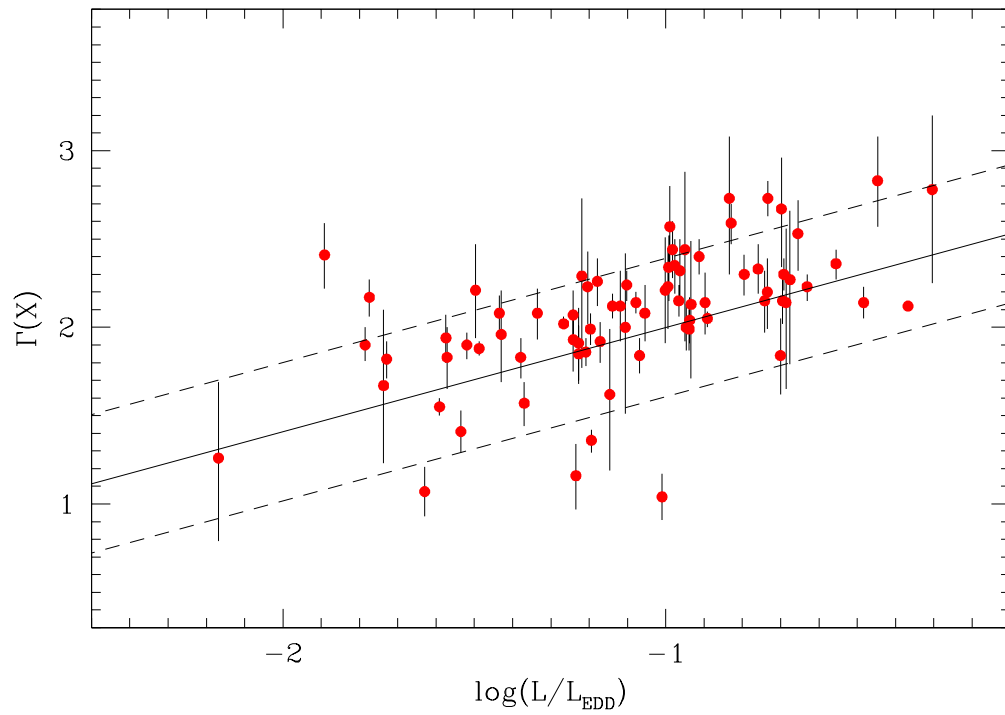


Fig. 2.— Correlations between Γ_X and L/L_{EDD} for the subsample of objects with black hole mass determined from the $H\beta$ line. This is the strongest correlation found in our analysis.

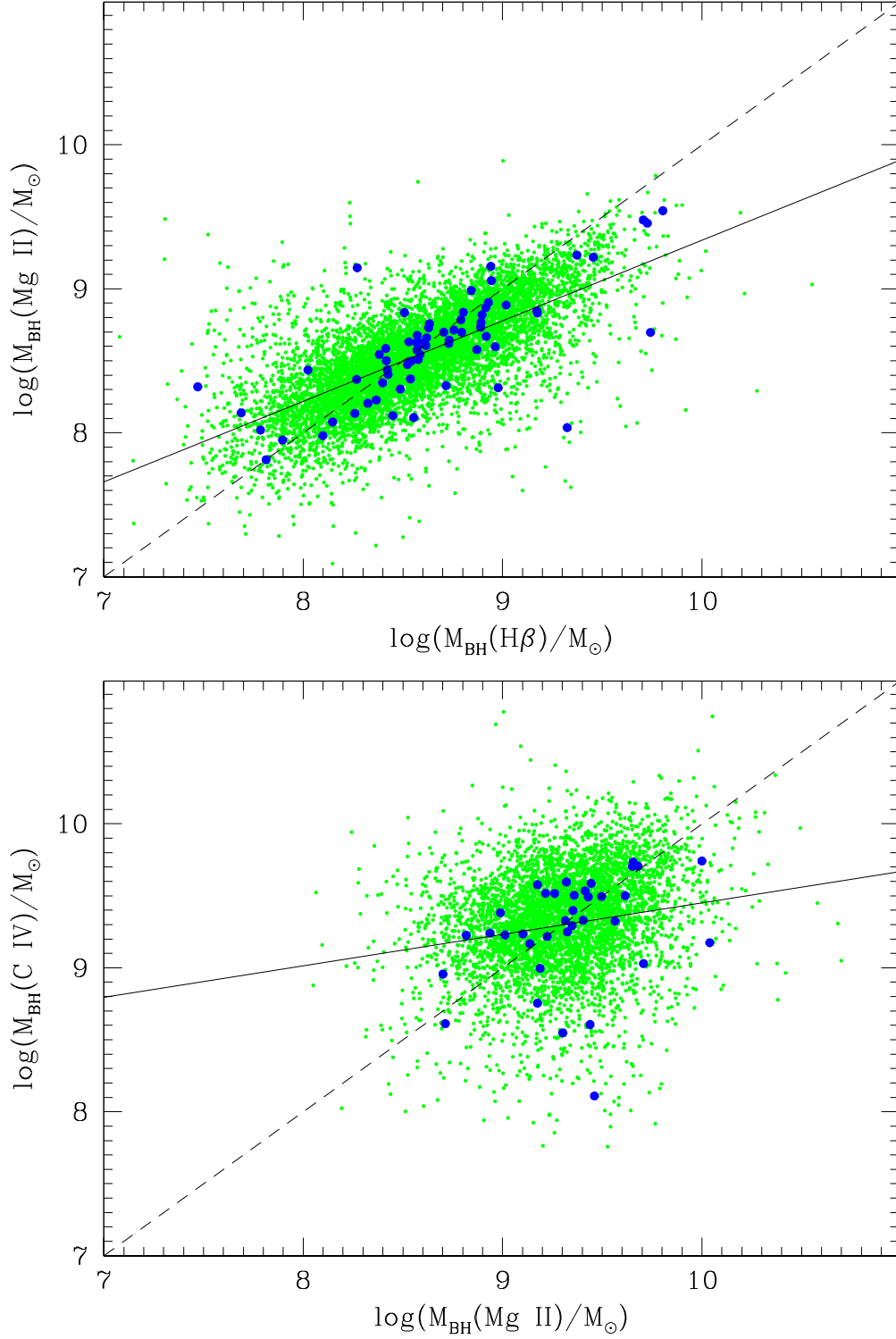


Fig. 3.— Comparison between the S08 black hole mass estimates from different lines. The blue points are the objects in the SDSS/XMM-Newton sample. The continuous lines show the linear best fits (though the linear correlation in the C IV-Mg II plane is barely significant, see text for details). The dashed lines indicate the one-to-one relation.